PCCP

Accepted Manuscript

ROYAL SOCIETY OF CHEMISTRY

www.rsc.org/pccp

Journal Name

ARTICLE

Efficient microfluidic photocatalysis in symmetrical metal-cladding waveguide

Received 00th January 20xx,
Accepted 00th January 20xx

DOI: 10.1039/x0xx00000x

www.rsc.org/

Shu Zhu, Hailang Dai, Bei Jiang, Zhenhua Shen and Xianfeng Chen*

In this paper, a symmetrical metal-cladding optical waveguide based microfluidic chip with self-organized, free-standing TiO_2 nanotube membrane is utilized to performing efficient photocatalysis. The chip has a microchannel bonding with TiO_2 nanotube coated glass. The employment of microfluidic chip for hydrolysis reaction can make the mass and photo transferred. Meanwhile the incorporation of the double metal-cladding waveguide enhances the light matter interaction and further effectively improves the efficiency of photocatalysis.

Introduction

With the rapid development of science and technology, profound changes have taken place in urban and rural areas. The demand and calls for curbing environmental pollution, enhancing the quality of life and construction of ecological civilization city are increasing. Particularly, environmental pollution is still quite serious on the whole, although the situation has improved in some areas after a long-term treatment. Currently, in order to improve the efficiency of environmental pollution control, more and more people have focused their eyes on using a variety of photocatalytic technology to deal with environmental pollution. Photocatalytic technology employs solar energy to conversion and utilization of energy, mechanistic organic photochemistry, environmental cleaning and so on. Many physical, chemical and environmental researchers take part in these aspects of study with the purpose of solving the obstacles of energy and environment.[1] As a common material used for photocatalysis, nano-TiO_2 attracts much attention due to its strong ability of oxidation, good stability, low cost and less contamination.[2-5]

The reported papers about photocatalytic reaction are usually carried out in a conventional batch reactor. The reaction volume usually ranges from a few millimeters to several tens millimeters, thus producing a lower reaction efficiency. In recent years, a type of photochemical reaction based on a continuous flow microreactor which is called microfluidic technology has been extensively studied. Microfluidic technology, as one of the most cutting-edge fields of science and technology, shows a tremendous prospect in bioscience, industrial synthesis and some other fields by virtue of its unique advantages such as good controllability, high-throughput and low-cost.[6] In addition, the microchannel in the chip has a very high specific surface area,[7] which makes the photon and mass transfer efficiently during photoreaction. Hence the efficiency of photocatalysis would be several times higher than conventional batch reaction.[7-11]

A reactor based on TiO_2-coated silica waveguide in an attenuated total reflection (ATR) mode for the photocatalytic oxidation of formic acid in water has been proposed in 1999.[12] This method could utilize light power more efficiently or enhance quantum efficiency.[13] During the ATR propagation, incident light upon the interface of silica/ TiO_2/ water is completely reflected back into the silica. In every process of reflection, the TiO_2 film absorbs more energy of UV light. Further improvement of photocatalysed effieciecy remains an important issue and attracts much attention.

When the incident light couples into the guiding layer at couple angle,[14] more than 1000 modes of ATR modes (ATRM) can be excited in symmetrical metal-cladding waveguide (SMCW).[15] Due to the strong optical energy confinement of SMCW, the Quality factor of (10^5)[16, 17] can be reached. So the incident light can obtain gratifying efficiency by high power density. In addition, the SMCW is also highly-sensitive to the incident wavelength. Here, we propose a novel microfluidic chip based on the SMCW to enhance the efficiency of photocatalysis. In order to demonstrate the feasibility of the device, methylene blue was selected as the model of organic wastewater. We also developed a model using Finite-Difference Time-Domain (FDTD) to simulate exemplarily a setup to permit for an estimation of the increase of light intensity in the microfluidic chip due to the presence of the SMCW.

Experimental

State Key Laboratory of Advanced Optical Communication Systems and Networks, Department of Physics and Astronomy, Shanghai Jiao Tong University, 800 Dongchuan Road, Shanghai 200240, China
E-mail: xfchen@sjtu.edu.cn

Fabrication of microfluidic chip based on SMCW

The chip structure is shown in Fig. 1. The microchannel in the microfluidic chip is fabricated by conventional soft lithography techniques. The sizes of the main channel area are 7 mm in length, 2.5 mm in width and 125 μm in height. Due to the high reflectivity in UV region, we choose Aluminium as metal-cladding layers. Aluminum film with the thickness of 20 nm was deposited on the top of this main channel area of the PDMS slab for better coupling. The aluminium film with the thickness of 300 nm was deposited at the bottom of the glass slab to prevent light leakage. Then the PDMS slab with membrane in its channel and a glass slide were placed into the plasma chamber and exposed oxygen plasma for permanent bonding. For comparison, microfluidic chip without SMCW was also fabricated in this work.

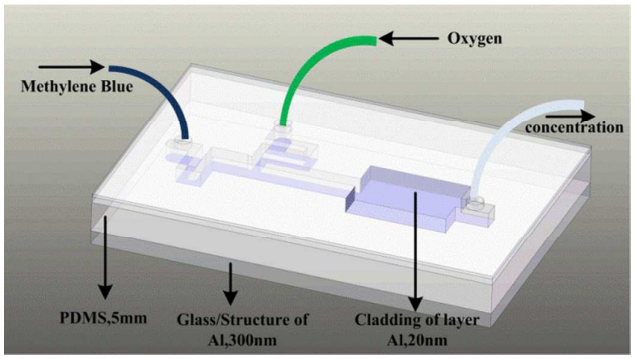

Fig. 1 Diagram of the microfluidic chip based on symmetrical metal-cladding waveguide

Preparation and characterization of TiO_2 nanotube membrane

The preparation method of TiO_2 nanotube membrane is discussed in our previous work.[18] In conclusion, TiO_2 nanotube membrane was obtained by anodic oxidation method. The Ti foils play as the working electrode and the Pt plays as the counter electrode. The Ti substrate was first treated in the electrolyte made of ethylene glycol, 3v% deionized water and 0.5w% ammonium fluoride at the working voltage of 60 V at room temperature for 1 h and then a surface layer of TiO_2 can be formed. After the removal of surface TiO_2, the substrate would be treated the second anodization for about 60 minutes at the same working voltage. Finally, the TiO_2 membrane was detached from the substrate after annealing in the furnace at 450 C^o for 2 h. Then the sample was sent to the scanning electron microscopy (SEM, NOVA NanoSEM230, FEI) for morphology analysis.

Photocatalytic degradation methylene blue

The effect of the photocatalytic degradation was evaluated by methylene blue (MB) as a model pollutant under the irradiation of UV lamp and the reaction equation was as follows:

$$2C_6H_{18}N_3SCl + 31O_2 \xrightarrow{TiO_2,hv} 2HCl + 2H_2SO_4 + 6HNO_3 + 12CO_2 + 12H_2O \quad (1)$$

The initial concentration of MB is about 0.15 g/L while the precise value would be detected by the ATR indicatrix. In a typical experiment, 5 mL of the above MB solution was injected through the inlet into the microfluidic chip using a syringe pump via tygon tubing and oxygen was injected through another inlet at the flow rate of 5 μL/ min.

Results and discussions

Simulation result

In order to verify the feasibility of the experiment, we build a model as is shown in Fig.2. A 20 nm aluminum film with an area of 7×2.5 mm^2 is used as the top cladding of the waveguide. The layer underneath is microchannel with a thickness of 125 μm which is full of MB solution. At the bottom of the microchannel, there is a piece of TiO_2 nanotube membrane with the thickness of 15 μm. Then, another 300 nm thick aluminum is added as the bottom cladding. The refractive index of solvent is 1.33 and the dielectric constant of TiO_2 is set to be 2.6. Based on the simulation，over 1000 modes can be obtained. The result of the simulation showing the optical power intensity distribution of the ultrahigh order modes inside the microchannel based on symmetrical metal-cladding waveguide is shown in Fig.3. The simulation results reveal one of the optical oscillating mode when the incident light wavelength is of 269.4 nm at the incident angle of 43.8°. Since the UV light source is focused by a convex lens in our experiment, the light is coupled into the waveguide through various incident angles and thus large portion of violet spectrum of the sunlight with phonon energies above the bandgap of TiO_2 can be efficiently coupled into the SMCWs under irradiation of the ambient sunlight.

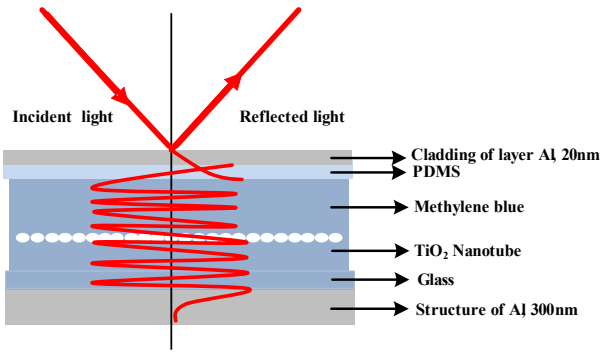

Fig. 2 Schematic diagram of the light coupling process in the symmetrical metal-cladding waveguide when photocatalytic degrading MB

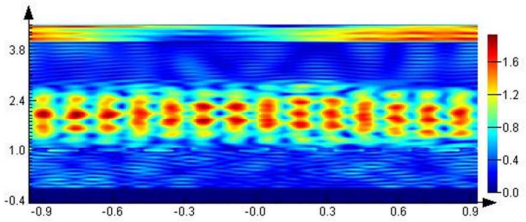

Fig. 3 FDTD simulation result of the increasing light intensity in the waveguide when photocatalytic degrading MB

Characterization

Fig. 4 shows the SEM picture of the annealed free-standing TiO_2 nanotube membrane. The top view of the membrane is shown in Fig. 4(a). The inner diameter of the nanotube is around 80 nm and the thickness of the nanotube is about 10 nm. Fig. 4(b) and Fig. 4(c) show the cross section of the TiO_2 nanotube membrane with the tube lengths of approximately 15 μm.

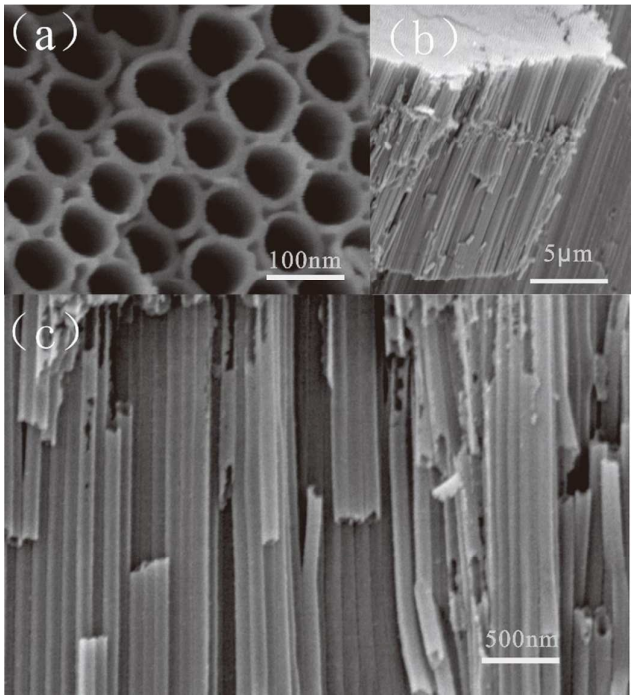

Fig. 4 SEM imagines of the TiO_2 nanotube membrane. (a) The top view of the nanotubes. (b) Cross section of the TiO_2 nanotube membrane. (c) Magnified cross section of the nanotube.

The action principle of SMCW[19, 20]

According to electromagnetic field boundary conditions, the reflectivity can be expressed as:

$$R_{\min} = |r_{12}|^2 \left[1 - \frac{4Im(\beta^0)Im(\Delta\beta^{\mathrm{rad}})}{\left(Im(\beta^0)+Im(\Delta\beta^{\mathrm{rad}})\right)^2}\right] \quad (2)$$

$$\beta^0 = k_0 N = k_0 n_0 \sin\theta \quad (3)$$

$$k_0 = 2\pi/\lambda \quad (4)$$

Where Im (β^0) and Im ($\Delta\beta^{\mathrm{rad}}$) are intrinsic and radiative loss respectively. β^0 is the propagation constant for an effective index N of the guided modes.

Im (β^0) represents the transmission loss which is correlated with the extinction coefficient of the waveguide. Im ($\Delta\beta^{rad}$) stands for the radiative loss of the guided wave which is highly associated with the thickness of the metal layer. κ_0 is the wavenumber of light with wavelength λ in free space, and θ is the incident angle. When Im (β^0) = Im ($\Delta\beta^{\mathrm{rad}}$), R_{min} becomes zero and the critical condition can be realized. Two methods can be applied to figure out the refractive index of the liquid guiding layer inside the symmetric metal cladding waveguide. One is to determine the real part of the complex refractive index of the analyte and the other is to determine the imaginary part of the complex refractive index. The variation in analyte concentration results in the change of refractive index of the solution, which also affects the resonance angle and the position of ATR tips. In addition, the depth of the dip will rise or fall according to the imaginary part of the complex refractive index. Whether the depth rises or falls relies on the discrepancy between the intrinsic and radiative damping.

Photocatalytic degradation performance of the microfluidic chip

The results of the degradation at the flow rate of 5 μL/min under the irradiation of UV lamp are tested by ATR shown in Fig. 5. Fig. 5(a) shows the depth of the dip at the coupled angle decreases from 1.5^0 to 3.5^0. There are black, red and blue curves, respectively represent initial, with waveguide and without waveguide method. Fig. 5(b) shows the minimum reflectivity and the concentration of MB, where the incident of angle between 2.25^0 to 2.40^0. As we know, the higher the concentration is, the higher the intrinsic loss is. Via equation (2) meanwhile, the higher intrinsic loss is, the smaller minimum reflectivity is. In conclusion, the effect of photocatalysis in the microfluidic chip with SMCW is the best.

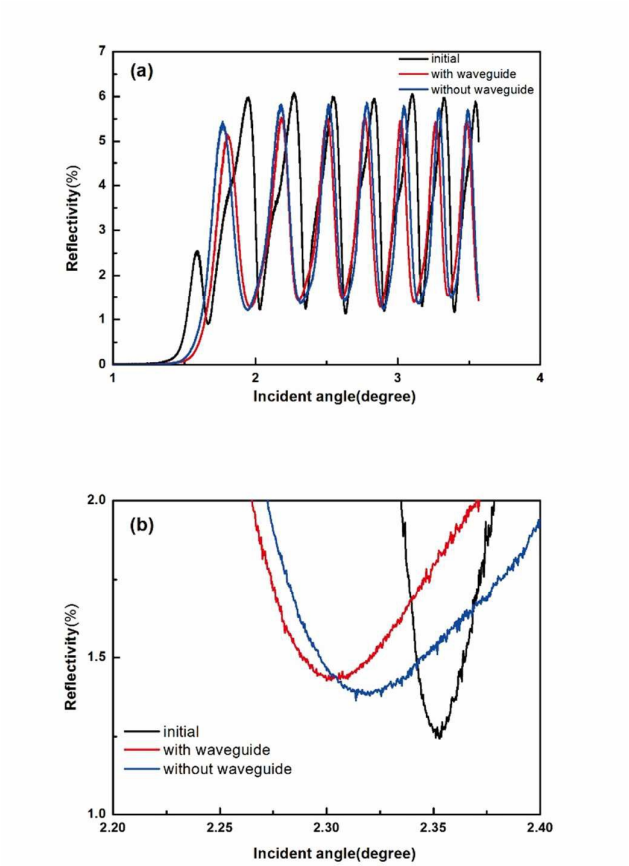

Fig. 5 ATR spectrum for initial MB solution and photocatalyzed MB solution in different microfluidic chips.(a) The depth of the dip at the coupled angle decreases from 1.5^0 to 3.5^0.(b) Magnified picture of the minimum reflectivity as a function of the concentration of MB, where the incident angle ranges from 2.25^0 to 2.40^0 .

Selecting five sets of data about concentration and minimum reflectivity from continuous peaks in Fig. 5(a) curve, and a set of data was input to calculate the refractive index of software to find refractive index on different concentrations. We can achieve the relation between the refractive index and solution concentration of mathematical expression. Table.1 shows the concentration of initial MB solution and photocatalyzed MB solution in different microfluidic chips. Original concentration of MB solution is 0.143 g/L. The concentration of MB solution turns to 0.053 g/L after traditional microfluidic photocatalysis process. The efficiency of photocatalysis increased by 40% with the help of SMCW and the final concentration is 0.017 g/L under the same flow rates in the microchannel.

Table.1 The concentration of initial MB solution and photocatalyzed MB solution in different microfluidic chips

Sample	Concentration(g/L)
Initial	0.143
Without waveguide	0.053
With waveguide	0.017

Conclusions

In conclusion, a microfluidic chip based on SMCW was proposed to realize efficient photocatalysis. The chip was manufactured by conventional soft lithography technique. Light intensity was largely enhanced due to the excitation of several oscillating modes in SMCW. Compared with traditional microfluidic photocatalysis, symmetrical metal-cladding waveguide based microfluidic photocatalysis demonstrated an increased efficiency of about 40%. Such symmetrical metal-cladding waveguide based microfluidic chip offers a great potential platform for efficient wastewater treatment.

Acknowledgements

This work was supported by the National Basic Research Program of China (No. 2011CB808101), the National Natural Science Foundation of China (No. 61125503), the National Basic Research Program of China (No. 2013CBA01703) and the Foundation for Development of Science and Technology of Shanghai (No. 13JC1408300).

Notes and references

1 1. M. N. Chong, B. Jin, C. W. Chow and C. Saint, *Water research*, 2010, **44**, 2997-3027.
2 2. V. Shapovalov, *Glass Physics and Chemistry*, 2010, **36**, 121-157.
3 3. J. M. Meichtry, H. J. Lin, L. de la Fuente, I. K. Levy, E. A. Gautier, M. A. Blesa and M. I. Litter, *Journal of Solar Energy Engineering*, 2007, **129**, 119-126.
4 4. M. Ni, M. K. Leung, D. Y. Leung and K. Sumathy, *Renewable and Sustainable Energy Reviews*, 2007, **11**, 401-425.
5 5. X. Zheng, D. Li, X. Li, L. Yu, P. Wang, X. Zhang, J. Fang, Y. Shao and Y. Zheng, *Physical Chemistry Chemical Physics*, 2014, **16**, 15299-15306.
6 6. D. Beebe, M. Wheeler, H. Zeringue, E. Walters and S. Raty, *Theriogenology*, 2002, **57**, 125-135.
7 7. G. Takei, T. Kitamori and H.-B. Kim, *Catalysis Communications*, 2005, **6**, 357-360.
8 8. H. Lu, M. A. Schmidt and K. F. Jensen, *Lab on a Chip*, 2001, **1**, 22-28.
9 9. R. C. Wootton, R. Fortt and A. J. de Mello, *Organic process research & development*, 2002, **6**, 187-189.
10 10. H. Lindstrom, R. Wootton and A. Iles, *AIChE journal*, 2007, **53**, 695-702.

11 11. R. Gorges, S. Meyer and G. Kreisel, *Journal of Photochemistry and Photobiology A: Chemistry*, 2004, **167**, 95-99.
12 12. A. L. Lawrence, K. M. McAloon, R. P. Mason and L. M. Mayer, *Environmental science & technology*, 1999, **33**, 1871-1876.
13 13. T. Xu, L. Huang, D. Wei, Y. Jin, J. Fang, G. Yuan, Z. Cao and H. Li, *Optics Communications*, 2014, **333**, 67-70.
14 14. W. Yuan, C. Yin, H. Li, P. Xiao and Z. Cao, *JOSA B*, 2011, **28**, 968-971.
15 15. J. Sun, C. Yin, C. Zhu, X. Wang, W. Yuan, P. Xiao, X. Chen and Z. Cao, *JOSA B*, 2012, **29**, 769-773.
16 16. X. Wang, C. Yin, H. Li, M. Sang, W. Yuan and Z. Cao, *Optics letters*, 2013, **38**, 4085-4087.
17 17. L. Xiang, C. Zhuang-Qi, S. Qi-Shun, M. Qing-Hua, H. De-Ying, G. Kun-Peng, Q. Ling and S. Yu-Quan, *Chinese Physics Letters*, 2006, **23**, 998.
18 18. S. Zhu, X. Liu, J. Lin and X. Chen, *Opt. Mater. Express*, 2015, **5**, 2754-2760.
19 19. H. Dai, M. Sang, Y. Wang, R. Du, W. Yuan, Z. Jia, Z. Cao and X. Chen, *Sensors and Actuators A: Physical*, 2014, **218**, 88-93.
20 20. H. Li, Z. Cao, H. Lu and Q. Shen, *Applied Physics Letters*, 2003, **83**, 2757-2759.
21